LOX DROPLET VAPORIZATION IN A SUPERCRITICAL FORCED CONVECTIVE ENVIRONMENT

Chia-chun Hsiao and Vigor Yang
Propulsion Engineering Research Center
Department of Mechanical Engineering
The Pennsylvania State University
University Park, PA 16802

SUMMARY:

A systematic investigation has been conducted to study the effects of ambient flow conditions (i.e. pressure and velocity) on supercritical droplet gasification in a forced-convective environment. The model is based on the time-dependent conservation equations in axisymmetric coordinates, and accommodates thermodynamic nonidealities and transport anomalies. In addition, an efficient scheme for evaluating thermophysical properties over the entire range of fluid thermodynamic states is established. The analysis allows a thorough examination of droplet behavior during its entire lifetime, including transient gasification, dynamic deformation, and shattering. A parametric study of droplet vaporization rate in terms of ambient pressure and Reynolds number is also conducted.

TECHNICAL DISCUSSION:

Many liquid-fueled combustion systems (such as diesel engines, ramjets, gas turbines and liquid rockets) are designed to deliver fuel and oxidizer into a pressurized chamber through atomizers which break the liquid fuel and form a large number of droplets. These droplets then undergo a series of vaporization, breakup, and mixing process to form fuel-oxidizer mixture for reaction. Modern combustor designs even extend the chamber operational condition into regimes well above the thermodynamic critical points of fuels for better performance. Information regarding droplet trajectory, breakup criteria, and gasification rate in a supercritical convective environments becomes crucial.

Although several studies have been conducted to investigate the characteristics of droplet vaporization in supercritical conditions (Hsieh *et al.*, 1991; Shuen *et al.*, 1992; Yang *et al.*, 1994), effects of ambient convective flow on droplet behavior have not yet been addressed. The purpose of the present work is to conduct a systematic investigation into supercritical droplet vaporization in a forced-convective stream. The formulation starts with the time-dependent conservation equations of mass, momentum, energy, and species concentration in axisymmetric coordinates for both droplet interior and ambient gases. Full account is taken of thermodynamic non-ideality and transport anomaly during the droplet phase transition from the subcritical to supercritical state. In addition, a unified property evaluation scheme based on the BWR equation of state and extended corresponding-state technique is established to predict fluid thermophysical properties. The governing equations and associated boundary conditions are solved numerically using an implicit finite-difference scheme with a dual time-stepping integration scheme.

In the first part of this study, a series of calculations has been carried out to study liquid oxygen (LOX) droplet gasification in a hydrogen stream at different pressures and Reynolds numbers. Detailed velocity and thermodynamic properties contours have been studied thoroughly. Secondly, a parametric study is conducted to establish correlations for droplet lifetime, gasification rate, and drag coefficient as functions of ambient pressure, temperature, droplet diameter and Reynolds number.

Governing Equation

The flow under consideration is laminar and axisymmetric. If body forces, viscous dissipation, and thermal radiation are ignored, the conservation laws can be written in the following form.

Mass:

$$\frac{\partial}{\partial t}\iiint \rho dV + \iint \rho u_j dA_j = 0. \tag{1}$$

Momentum:

$$\frac{\partial}{\partial t}\iiint \rho u_i dV + \iint \rho u_i u_j dA_j = \iint \tau_{ij} dA_j. \tag{2}$$

Energy:

$$\frac{\partial}{\partial t}\iiint \rho e dV + \iint \rho e u_j dA_j = \iint \tau_{ij} u_i dA_j - \iint (q_T)_j dA_j. \tag{3}$$

Species Concentration:

$$\frac{\partial}{\partial t}\iiint \rho Y_l dV + \iint \rho Y_l u_j dA_j = -\iint (q_{M,l})_j dA_j. \tag{4}$$

where

$$\tau_{ij} = -p\delta_{ij} + 2\mu e_{ij} - \frac{2}{3}\mu(\nabla \cdot u)\delta_{ij}.$$

Standard notations in fluid mechanics and thermodynamics are used in (1)-(4). The specific total energy e at a given pressure is defined as

$$e = \sum_{l=1}^{N} Y_l (h^0_{f,l} + \int_{T_{ref}}^{T} C_{p,l} dT) - \frac{p}{\rho} + \frac{u_i u_i}{2},$$

where the index N represents the number of species considered, Y_l the mass fraction of species l, and T_{ref} the reference temperature for enthalpy of formation. Fick's and Fourier's laws are used to approximate the species and thermal diffusion in Eqs. (3) and (4), respectively.

Property Evaluation

An extended corresponding-state principle, which requires only critical constants and Pitzer's acentric factor for each component, is used to predict properties over the entire range of fluid p-v-T states for a mixture. The basic idea of the corresponding state model is relatively straightforward. It is assumed that the configurational properties of a single-phase mixture can be adequately represented by those of a hypothetical pure fluid. The properties of this hypothetical pure fluid are then evaluated via corresponding states with respect to a given reference fluid. The extended corresponding-state theory using shape factors and mixture combining rules can satisfactorily predict the thermodynamic properties of mixtures from an equation of state of the reference substance. Meanwhile, transport properties are expressed as a function of density and temperature through conformal mapping to the reference fluid. For accurate property prediction, it is desirable to have an equation of state that accurately represents the p-v-T behavior of a mixture.

In the present study of multicomponent droplet dynamics at supercritical conditions, a generalized *BWR* equation of state is used to predict both gas and liquid phase behavior of the reference fluid.

$$p = \sum_{n=1}^{9} a_n(T)\rho^n + \sum_{n=10}^{15} a_n(T)\rho^{2n-17} e^{-\gamma\rho^2} \tag{5}$$

where γ is 0.04, and the functional coefficients $a_n(T)$ vary with the reference fluid. This equation of state must be solved iteratively to obtain the density of the reference fluid. The density of the mixture is then obtain through an extended corresponding-state method.

$$\rho = \frac{\rho_0[T/f_{m,0}, p(h_{m,0}/f_{m,0})]}{h_{m,0}} \tag{6}$$

Enthalpy, internal energy, entropy, fugacity, etc., are important thermodynamic properties, which can be related to engine operating variables such as temperature and density. The heat capacity of a mixture can be expressed as the sum of the ideal gas heat capacity at the same temperature and composition plus a residual heat capacity (Leach, 1967)

$$C_p = C_p^0 + \Delta C_p \tag{7}$$

where ΔC_p is most conveniently determined by

$$\Delta C_p = T \int_{\infty}^{V} (\frac{\partial^2 p}{\partial T^2}) dV - \frac{T(\partial p/\partial T)_V^2}{(\partial p/\partial V)_T} - R$$

Viscosity coefficient for a mixture fluid can be reproduced using a two-shape-factor corresponding-state method with correction for mass and size difference.

$$\mu_{mix}(\rho, T, \{x_a\}, \{m_a\}) = \mu_0(\rho_0, T_0) F_\mu + \Delta\mu^{ENSKOG} \tag{8}$$

where

$$F_\mu = \left(\frac{M_m}{M_0}\right)^{1/2} f_{x,0}^{1/2}\ h_{x,0}^{-2/3}$$

Here M_m is the molecular weight of the mixture. A relatively simple correction taken from the Enskog hard sphere theory is used with the predictions. The function corrects for deviations in mass mixing rules at low densities, and for differences in molecular size.

$$\Delta\mu^{ENSKOG} = \mu_{mix}^{ENSKOG}(\{\rho\sigma_a^3\}, \{x_a\}, \{m_a\}) - \mu_x^{ENSKOG}(\rho\sigma_x^3, m_x) \tag{9}$$

The Enskog model (1954) has been solved for a multicomponent mixture of hard spheres by Tham and Gubbins (1971) and is used to calculate μ_{mix}^{ENSKOG} and μ_x^{ENSKOG}.

Ely and Hanley proposed an expression for thermal conductivity which can be divided into three contributions,

$$\lambda = \lambda'(\rho, T) + \lambda''(T) + \Delta\lambda_{crit}(\rho, T) \tag{10}$$

The first term on the right-hand side is caused by the transfer of energy from purely collisional or translational effects and can be calculated via the corresponding-state method. The second term in Eq. (10) is due to the transfer of energy via internal degrees of freedom. This is independent of density and may be evaluated by the modified Eucken correlation with an empirical mixing rule for polyatomic gases. Modern theory of transport phenomena (Sengers,1971,1972) predicts an infinite thermal conductivity at the pure fluid critical point and a large enhancement of thermal conductivity in the vicinity of the critical point. The third term in Eq. (10) accounts for this phenomenon and is a function of temperature and density.

RESULTS:

The theoretical model described in the preceding sections has been applied to LOX droplet vaporization in a hydrogen stream at different pressures (100, 200 and 400 atm) and Reynolds numbers ($60 - 250$). A LOX droplet with initial temperature of 100 K and introductory diameter of 100 μm is injected into the 1000 K hydrogen stream. Part of the heat transferred from the gas phase goes into vaporizing droplet, while the remainder goes into heating the droplet interior. Since the critical mixing temperature of oxygen is 154.6 K at 1 atmosphere and decreases with increasing pressure, the droplet becomes supercritical almost instantaneously upon introduction to the hydrogen gas at the supercritical pressure levels of interest (100, 200 and 400 atm). Once this occurs, the enthalpy of vaporization and surface tension vanish, leaving an essentially continuous medium with no abrupt phase change in the vaporization process. Although the interior region of the droplet remains at the liquid state with a subcritical temperature distribution, the medium attributes (ρ, p, T and thermophysical properties) vary continuously between the liquid core and ambient gases with no distinct liquid surface as exists for a droplet in a subcritical environment. As a result, a single-phase analysis is used to treat the droplet interior and ambient gases simultaneously as one fluid. Since there is no discontinuity, the surface of the droplet is defined as the surface at which the temperature attains the value of the critical mixing temperature.

Density contours with streamline patterns are shown in Fig. 1 for the 5 m/s ambient flow case considered here. A recirculating flow in the wake of the droplet occurs as a result of the shear force between liquid oxygen and the surrounding gases. For the higher Reynolds number case (15 m/s), droplet shattering is seen, as shown in Fig. 2. The convective flow penetrates through the liquid phase, breaking the droplet into two parts - the core disk and the surrounding ring. The wake region, however, is convected away from the droplet due to the diminishing shear flow between gas and liquid phases. In both of these supercritical cases, no discernible flow circulation is found in the droplet interior, in contrast to the Hill's vortex found in low-pressure cases.

Time variations of droplet residual mass at different pressures and velocities are shown in Figs. 3 and 4. When droplet surface reaches critical condition, no sharp boundary between gas and liquid phases exists. The entire flow field becomes a continuous medium. Under this condition, droplet vaporization is best characterized by the droplet residual mass which is confined by a surface with critical mixing temperature. Results show that high Reynolds number favors droplet evaporation. In a stronger convective flow (15 m/s), droplet tends to deform and as such increases contact surface with ambient flow, while the ambient stream convects the gasified oxygen downstream and enhances both thermal and species diffusion. Figures 5 and 6 show the time variations of droplet moving velocity. The first derivative of these curves can be used to calculate droplet acceleration. Drag force defined by Newton's second law can be obtained by multiplying acceleration of center of gravity with its mass.

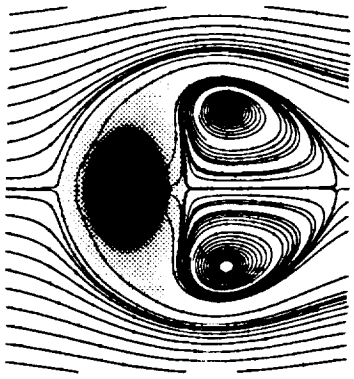

Figure 1: Density Contours and Streamlines at $t = 176\mu s$, LOX/H_2 System, $D_0 = 100\mu m$, $p_\infty = 100$ atm, and $U_\infty = 5m/s$.

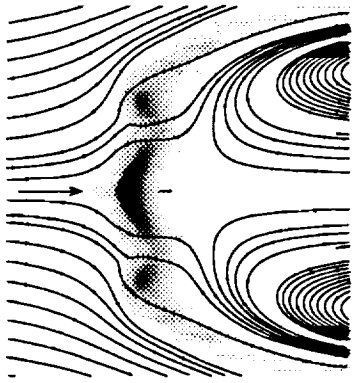

Figure 2: Density Contours and Streamlines at $t = 176\mu s$, LOX/H_2 System, $D_0 = 100\mu m$, $p_\infty = 100$ atm, and $U_\infty = 15\ m/s$.

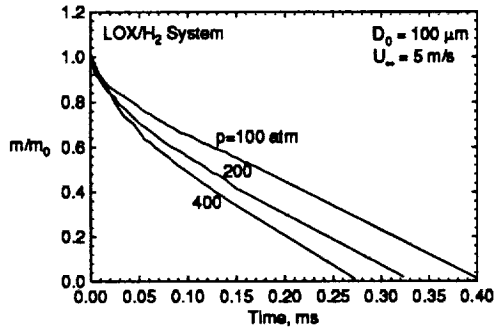

Figure 3: Time Variations of Droplets Residual Mass at Various Pressures, LOX/H_2 System, $D_0 = 100\mu m$, and $U_\infty = 5\ m/s$.

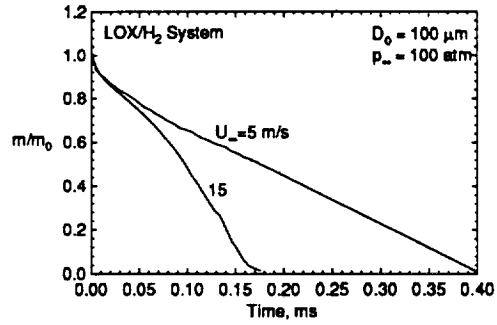

Figure 4: Time Variations of Droplet Residual Mass under Various Convective Velocities, LOX/H_2 System, $D_0 = 100\mu m$, and $p_\infty = 100$ atm.

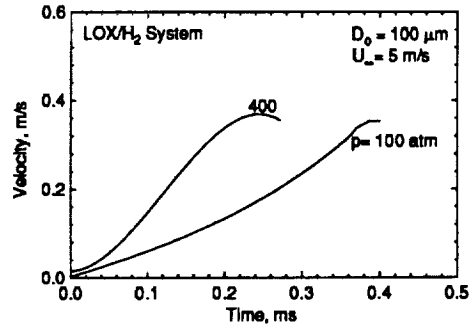

Figure 5: Time Variations of Velocity of Center of Gravity for Oxygen at Various Pressures, LOX/H_2 System, $D_0 = 100\mu m$, and $U_\infty = 5\ m/s$.

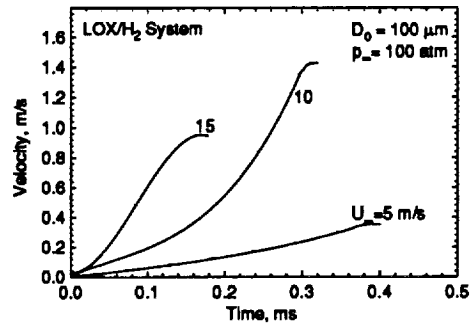

Figure 6: Time Variations of Velocity of Center of Gravity for Oxygen under Various Convective Velocities, LOX/H_2 System, $D_0 = 100\mu m$, and $p_\infty = 100$ atm.